# Detection of vesicant-induced upper airway mucosa damage in the hamster cheek pouch model using optical coherence tomography

**Marie J. Hammer-Wilson**
**Vi Nguyen**
**Woong-Gyu Jung**
**Yehchen Ahn**
**Zhongping Chen**
**Petra Wilder-Smith**
University of California
Beckman Laser Institute and Medical Clinic
1002 Health Sciences Road
Irvine, California 92612

**Abstract.** Hamster cheek pouches were exposed to 2-chloroethyl ethyl sulfide [CEES, half-mustard gas (HMG)] at a concentration of 0.4, 2.0, or 5.0 mg/ml for 1 or 5 min. Twenty-four hours post–HMG exposure, tissue damage was assessed by both stereomicrography and optical coherence tomography (OCT). Damage that was not visible on gross visual examination was apparent in the OCT images. Tissue changes were found to be dependent on both HMG concentration and exposure time. The submucosal and muscle layers of the cheek pouch tissue showed the greatest amount of structural alteration. Routine light microscope histology was performed to confirm the OCT observations. 
[DOI: 10.1117/1.3309455]

Keywords: 2-chloroethyl ethyl sulfide; half-mustard gas; vesicants; optical coherence tomography; hamster cheek pouch model; oral mucosa.

Paper 09155RR received Apr. 22, 2009; revised manuscript received Dec. 7, 2009; accepted for publication Dec. 8, 2009; published online Feb. 18, 2010.

## 1 Introduction

First used in World War I, vesicants ("blister agents") are the chemical warfare agents most commonly used against soldiers in combat.[1–3] The majority of the vesicants used as chemical warfare agents are alkylating compounds known as mustards.[3–6] They are easy to manufacture, store, and disperse. These lipophilic agents are difficult to protect against, as they readily penetrate epithelial surfaces such as skin and mucosa. Exposure causes cellular damage and/or cell death at the site of contact and at distant sites reached by the circulatory system, which they pass through before being eliminated in the subject's urine. Use of the vesicant with the greatest military importance, di(2-chloroethyl) sulfide (sulfur mustard or mustard gas), has been documented as recently as 1988. Following vesicant exposure, thorough and frequent patient examination is necessary to allow evaluation of injury progression or to monitor therapy response.

Of the major organs most affected by exposure to vesicants—the skin, eyes, and respiratory tract—the respiratory tract is the one that sustains the greatest, longest lasting damage.[7,8] However, the effects of vesicant exposure may not immediately be evident. Upper respiratory tract exposure to aerosolized mustard gas is usually followed by a latent or clinically asymptomatic period lasting from 0 to 24 h referring to Ref. 3, although in some instances, damage may lead to immediate bronchospasm.[9] Irritation, hoarseness, coughing, tracheobronchitis, airway obstruction, and in severe cases, hemorrhagic pulmonary edema are "acute" complications that manifest themselves over time, ranging from hours to as much as eight days post-exposure.[3,6] While the eye and skin can be monitored noninvasively by gross visual observation, most of the respiratory tract can be observed only by bronchoscopy. Noninvasive monitoring of the progression of injury or of the response to therapy is precluded using existing techniques. The need for noninvasive detection and monitoring of vesicant effects in the airway is further underlined by the fact that exposure to vesicants typically occurs on the battlefield, where bronchoscopy is not possible, yet accurate diagnosis of treatment needs, especially for immediate triage, is crucial.

Optical coherence tomography (OCT) is a noninvasive imaging technology that provides information about surface and subsurface tissue structure at discrete spatial locations in highly scattering biological tissues such as those found in the mouth and airway.[10–12] The high spatial resolution (2 to 10 $\mu$m) of OCT permits real-time near-histologic level "optical biopsy."[10,13–15] Using rapid-acquisition, high-resolution flexible fiber-optic probes, noninvasive OCT imaging of the upper airway (nose, mouth, and trachea) is possible. It is currently under investigation for a host of oral diagnostic applications, ranging from oral cancer to periodontal disease and decay. Thus, repeated noninjurious examination, monitoring, and evaluation of tissue status and treatment response in a patient is feasible. Upper airway OCT imaging may also provide information indicative of lower airway injury, avoiding invasive bronchoscopy procedures. These capabilities could lead to improved patient care and recovery.

Because of the toxicity of mustard gas, its common research analog, 2-chloroethyl ethyl sulfide [CEES, half-mustard gas (HMG), and half-sulfur mustard], is often used for laboratory tests. HMG is a monofunctional derivative of sulfur mustard that is less toxic,[16] but produces similar blis-

Address all correspondence to: Petra Wilder-Smith and Zhongping Chen, Beckman Laser Institute, University of California, Irvine, 1002 Health Sciences Rd., Irvine, California. Tel: 949-824-7632, Fax: 949-824-8413; E-mail: pwsmith@uci.edu or z2chen@uci.edu

1083-3668/2010/15(1)/016017/5/$25.00 © 2010 SPIE

tering lesions on the epithelial surface and has been shown to produce mustard gas–like response in rat lung.[17,18] HMG is also less environmentally persistent than mustard gas due to its being readily degraded upon contact with large volumes of water.[19] Thus, it can be handled using normal laboratory precautions.

The hamster cheek pouch (HCP) provides a good model for human oral mucosa. It has been the standard animal model used for this purpose for over 40 years.[20] In this study, topical exposure of the HCP to HMG was used to mimic exposure of the human oral cavity to chemical warfare agents.

The aim of this study was to investigate the use of noninvasive optical coherence tomography imaging techniques to detect changes in the hamster oral mucosa following half-mustard gas exposure. Our long-term goal is to develop a tool for monitoring the status of the entire airway based on noninvasive imaging of the more readily accessible upper airway.

## 2 Materials and Methods

### 2.1 *Vesicant*

2-chloroethyl ethyl sulfide (CAS 693-07-2) was purchased from Sigma Chemical (Cat. No. 242640, St. Louis, Missouri). Just prior to application, the commercial solution (5 mg/ml) was diluted to the desired exposure concentration of 0.4, 2, or 5 mg/ml in normal saline.

### 2.2 *Animal/Tissue Handling*

Nineteen male Golden Syrian hamsters (100+ g) were purchased from Harlan-Sprague Dawley Laboratories (Madison, Wisconsin) and divided into six groups: two animals at each exposure time for the low and mid-HMG concentrations, and five at 1-min and six at 5-min exposure time for the highest concentration. More animals were included in the higher exposure groups because of the heightened risk of animal death during the study. The animals were anesthetized using ketamine (200 mg/kg) and xylazine (10 mg/kg). One cheek pouch for each animal was everted over a cylindrical form and cleansed of debris using normal saline, and two small sutures of 7-0 Prolene monofilament (#8701 Ethicon, Inc., Piscataway, New Jersey) were placed at the base of the area to be treated. Each cheek pouch was treated topically with one of three concentrations of HMG—0.4, 2, or 5 mg/ml—for either 1 or 5 min. Application was accomplished by placing a 1 $cm^2$ gauze pad (Nu Gauze sponges, Johnson & Johnson Medical, Inc., Arlington, Texas) saturated with 0.5 ml of HMG solution on the HCP surface to mimic aerosol deposition in the oral cavity. Following HMG exposure, the area was rinsed with 100 ml of warm normal saline. Buprenorphine (0.5 mg/kg) was administered, and the animals were hydrated by subcutaneous injection of normal saline prior to recovery in an incubator. Once fully ambulatory, the hamsters were returned to their cages with free access to water but not food, to prevent mechanical damage to the cheek pouch tissue.

Twenty-four hours after HMG exposure, the animals were sacrificed by intracardiac injection of Eutha-6 (pentobarbital sodium, Western Medical Supply Co., Inc., Arcadia, California). The HMG-treated tissue was excised, pinned to cork, and fixed in 10% buffered formalin. An untreated area of the same cheek pouch was similarly fixed to serve as an internal control.

All experiments were carried out in accordance with the Institutional Animal Care and Use Committee at the University of California, Irvine, and were consistent with federal guidelines. Animals were treated in accordance with ARC guidelines at UCI (IACUC approval 2004-2547).

### 2.3 *Imaging and Histology*

Gross visual inspection of the fixed tissues was performed using an Olympus SZH stereomicroscope (Olympus America, Center Valley, Pennsylvania) at 10× prior to OCT imaging. Images were captured using a MIcroFire digital camera (Olympus America).

OCT imaging was performed on both HMG exposed and nonexposed areas using a frequency domain OCT system that has been previously described.[10] Four-mm-long, 2-D scan lines laterally centered in the application area were obtained at approximately 3 mm and 7 mm above the suture placement points on the HMG-treated samples. The position of the acquired images, indicated by the system locator beam, was marked with pins to allow relocation for comparison to histological sections. Randomly selected control areas from each cheek pouch were also scanned and marked.

After imaging, the cheek pouch tissue was processed for routine light microscope histology using an ATP-1 tissue processor (Triangle Biomedical Sciences, Durham, North Carolina), serially sectioned at 6 microns and H&E stained. OCT and histological images were matched to allow comparison of the structural features visualized by both techniques. Accurate co-localization of images was confirmed using anatomical landmarks such as blood vessels. Only where OCT images and histological sections could be positively matched was data analysis performed. Tissue measurements were performed under blinded conditions.

### 2.4 *Data Analysis*

Mean tissue thickness ± scanning electron microscopy was determined from the OCT images using IP Lab software (Scanalytics, Inc., Fairfax, Virginia). Individual layers of the HCP tissue were also identified on the OCT images and their thickness similarly measured. Student *t*-tests were performed to determine whether the differences observed in the tissues subsequent to the various HMG treatments were statistically significant.

## 3 Results

### 3.1 *Effects of HMG Visible to the Naked Eye*

Twenty-four hours post–HMG exposure, the excised cheek pouch tissue was examined using a stereomicroscope (Fig. 1). The lowest HMG concentration (0.4 mg/ml) evoked no visible response in the cheek pouch tissues. Slight blistering and increased membrane cloudiness were induced by 1- and 5-min exposure to 2 mg/ml of HMG. Gross examination of the cheek pouch tissue showed extensive visible response (blistering, membrane opacity, broken vessels) after 1-min and 5-min application durations at the highest HMG concentration (5-mg/ml).

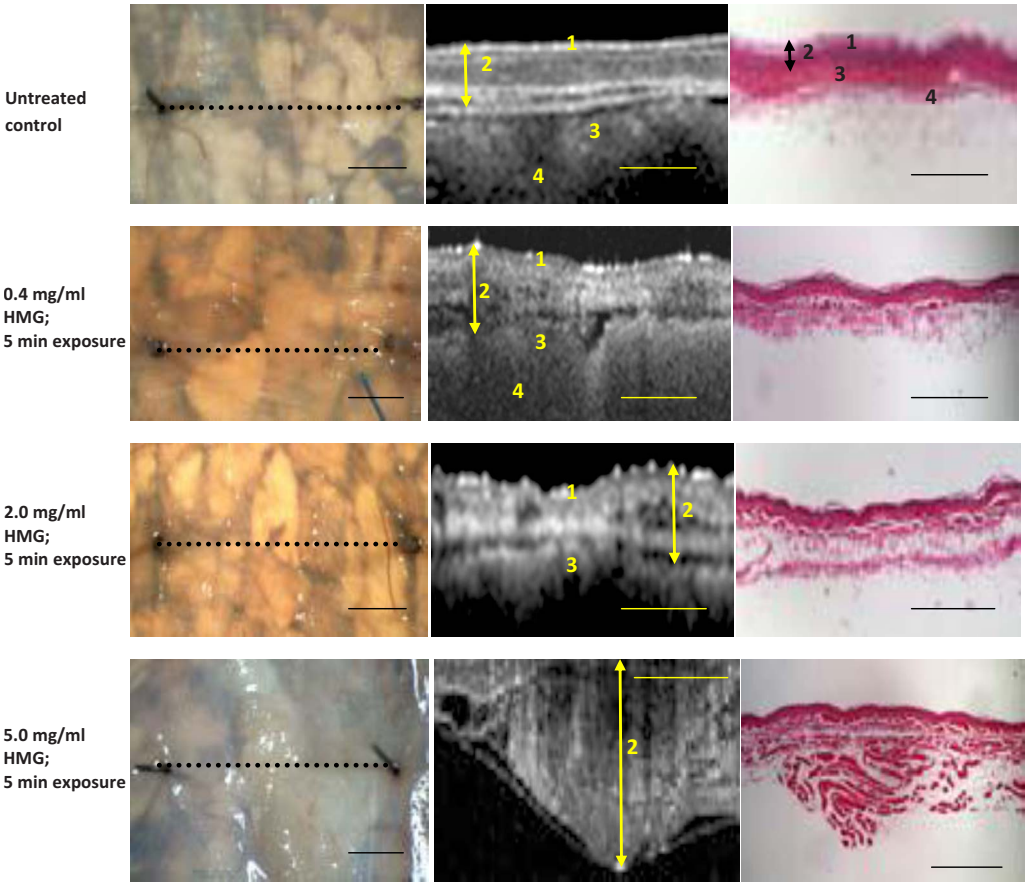


**Fig. 1** Stereomicrographs, OCT images, and corresponding histology of HMG treated hamster cheek pouch. Stereo micrographs (left column): Black dotted line=OCT imaging line. Arrows indicate visible blistering. OCT images (center column) and histological sections (right column): Double-ended arrow=maximum tissue depth of the mucosa. Total tissue thickness exceeds capturable OCT image size at the highest HMG concentration; surface epithelial layers are not visible in the OCT image. 1—Keratinized surface layer. 2—Flat stratified squamous epithelium. 3—Submucosa: dense fibrous connective tissue. 4—Longitudinal striated muscle. Calibration bars=1 mm.

### 3.2 *Effects of HMG Observed Using OCT and Histology*

Data from *in vivo* OCT imaging paralleled that obtained from histological slides of the same tissues viewed by conventional light microscopy (Fig. 1). Table 1 gives the mean total tissue thickness (± SEM) as measured on the OCT images. Based on the measurements made in Table 1, Fig. 2 shows that both HMG concentration and duration of exposure are important factors in inducing tissue response. Although there is a large amount of overlap in the degree of tissue response to the various treatments, the trends are clearly evident.

Examination of the characteristics of the individual tissue layers in the OCT images showed that the effects of HMG exposure were not uniformly distributed throughout the mucosa. Fairly modest, uneven increases in muscle fiber layer thickness were evident with 0.4 mg/ml HMG, with approximately 20% increases in tissue thickness at the shortest exposure time. Moderate structural damage was observed in the muscle fiber layer after exposure to 2.0 mg/ml HMG. Considerable irregular thickening and severe disruption of the muscle fiber layer resulted from 5.0 mg/ml HMG exposure. Typically, tissue thickness increased by >30% after HMG exposure at this level. HMG effects were localized primarily in the submucosa and muscle fiber layer of the mucosa (Fig. 3). More severe forms of damage caused a split within the muscle itself, with adhesion of the surface muscle layer to the overlying epithelial tissues and anchoring of the deeper muscle layers to the underlying structures. Exposure times of

**Table 1** Effects of HMG concentration and exposure duration on total tissue thickness.

| HMG exposure | Images analyzed | Mean tissue thickness (μm)±SEM | *P* value (compared to control) |
|---|---|---|---|
| None (control) | 10 | 265.8±14.6 | |
| 0.4 mg/ml; 1 min | 4 | 318.8±13.0 | 0.08 |
| 0.4 mg/ml; 5 min | 4 | 360±44.4 | 0.02 |
| 2.0 mg/ml; 1 min | 4 | 335.3±43.1 | 0.07 |
| 2.0 mg/ml; 5 min | 4 | 382.2±33.7 | 0.003 |
| 5.0 mg/ml; 1 min | 10 | 348.9±31.8 | 0.03 |
| 5.0 mg/ml; 5 min | 12 | 394.9±31.7 | 0.007 |

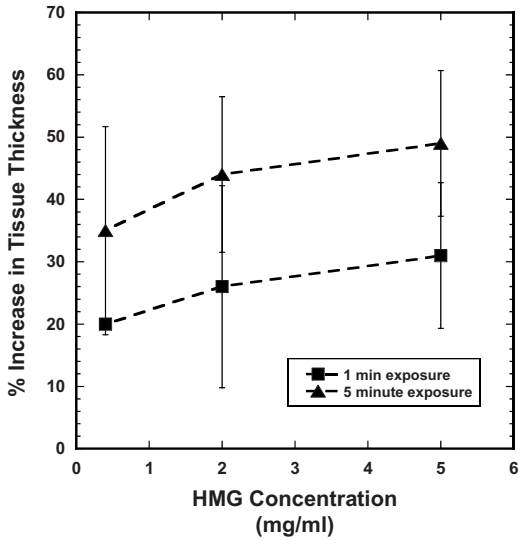


**Fig. 2** Tissue response to HMG exposure. Percent increase in total tissue thickness as a function of HMG concentration for 1-min and 5-min exposure times. Data points are mean±SEM.

1 min and 5 min appeared to produce similar degrees of damage for a given HMG concentration when grossly examined. OCT images, however, reveal that there can be extensive subsurface damage that is not apparent to the naked eye.

## 4 Discussion

Chemical warfare agents in general, and vesicants in particular, remain a concern of soldiers in combat. Of the major organs most commonly affected, the respiratory system is the least accessible, making it the most difficult in which to assess damage and to monitor treatment response. The purpose of our study was to determine whether noninvasive OCT imaging techniques are capable of detecting changes in the upper airway using HMG exposure concentrations that correlate with those found to produce damage in the lungs.

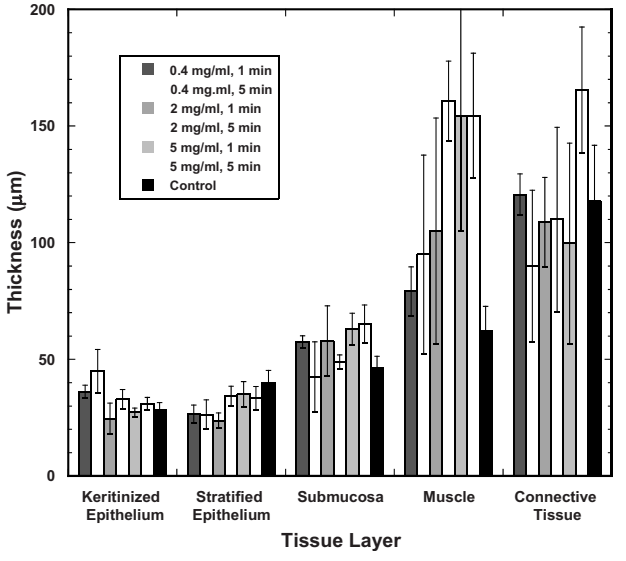


**Fig. 3** Tissue response by layer type. Thickness of each tissue layer of the hamster cheek pouch as measured on the OCT images following the application of HMG under various conditions. Values are mean±SEM.

Previously, most studies on the respiratory effects of mustard gas exposure have focused on the lower airway in rodents.[17,21–24] Two groups of researchers have conducted studies to determine how much HMG directly introduced into the lungs of rats will produce measurable damage. Anderson et al.[22] studied the pathological changes seen in the lung following exposure to HMG. McClintock et al.[17,18] explored the use of antioxidants as an antidote for injury induced by HMG. The HMG doses used in those studies ranged from a low of 0.35 mg/animal[22] to a maximum of approximately 4 mg/animal.[17] Based on data from inhalation studies in humans[25] and rats,[26] as well as deposition estimates from "The new ICRP respiratory tract and systemic models,"[27] it is reasonable to assume that approximately 3 to 5 times as much HMG is retained in the oral cavity as reaches the lungs. Thus, in order for the directly applied doses to have reached the lungs as a result of inhalation, the amounts retained in the animals' oral cavities in the McClintock et al. and Anderson et al. studies[17,22] would have been expected to be between 1 mg and 20 mg/animal. The lesser of these amounts is well above the lowest exposure concentration of 0.2 mg/animal used in our study. Even the highest amount used in our work, 2.5 mg/animal, falls in the lower portion of the range of concentrations directly applied by McClintock et al.[17] to induce measurable changes in the lungs. This demonstrates not only that OCT imaging is capable of detecting HMG exposure in oral mucosa, but also that it can do so at or even below levels expected to result in respiratory damage. Since the focus of this study was to testing the feasibility of using the OCT technique as a diagnostic tool and not to determine its optimum detection capability, establishing the lowest level of HMG exposure detectible was not undertaken.

Other studies in the rodent lung have shown that biochemical[17,18,28] and ultrastructural changes[17,29] can be detected as early as 4 and 6 h post–HMG exposure, respectively. In this first study, we chose to examine the single post-exposure time-point of 24 h because it is the generally accepted maximum length of time needed for symptoms to begin to become manifest.[3,6] Therefore, we cannot presently say exactly when after HMG exposure OCT imaging can detect changes in the mucosa. Another series of experiments will be focused on determining the earliest time-point at which HMG exposure can be reliably detected using OCT imaging.

This study shows that noninvasive OCT imaging can provide an accurate indication of damage to the upper airway after HMG exposure. Moreover, relatively minor changes not visible to the naked eye can be detected, and the level of tissue damage detected by imaging is commensurate with HMG exposure dose. Exposure to higher HMG concentrations for extended durations produced an increased reaction as manifested by overall tissue thickness. Moreover, it appears that a graduated tissue response to increasing dose and exposure duration was far more apparent in the deeper tissue layers (especially muscle and connective tissue) than in the superficial layers. In the epithelium, response to exposure was fairly similar for all doses. While the approach described in this paper served reasonably well to identify trends, the results of

this paper demonstrate that future imaging studies might benefit from the use of optical mapping techniques for more accurately documenting vesicant effects in specific tissue layers. Thus, OCT techniques may provide a means of detecting HMG-induced tissue damage and of monitoring the effectiveness of any attempted therapeutic interventions. This diagnostic capability would be of great benefit to both medical personnel and patients in managing instances of sulfur mustard, or other vesicant, exposure.

## 5 Conclusion

Noninvasive OCT can be used to visualize vesicant-induced damage in oral mucosa at or below exposure concentrations that have been shown to induce damage in the lower airway.

### *Acknowledgments*

The authors would like to thank Hongrui Li for assistance with histology and Hilari Kawakami-Wong for assistance with data analysis. This material is based on research sponsored by the Air Force Research Laboratory, under Agreement No. FA9550-04-1-0101. Additional support was provided by CA TRDRP 14IT-0097 NIH (LAMMP) RR01192, DOE DE903-91ER 61227, NIH EB-00293 CA91717, and NSF BES-86924.

### *References*

1. J. A. F. Compton, *Military Chemical and Biological Agents: Chemical and Toxicological Properties*, pp. 5–17, Telford Press, Caldwell, NJ (1998).
2. H. Sohrabpour, "Clinical manifestations of chemical agents on Iranian combatants during the Iran-Iraq conflict," *Arch. Belg.* 291–297 (1989).
3. R. N. Saladi, E. Smith, and A. N. Persaud, "Mustard: a potential agent of chemical warfare and terrorism," *Clin. Exp. Dermatol.* **31**, 1–5 (2005).
4. G. P. Wheeler, "Studies related to the mechanisms of action of cytotoxic alkylating agents: a review," *Cancer Res.* **22**, 651–688 (1962).
5. J. C. Dacre and M. Goldman, "Toxicology and pharmacology of the chemical warfare agent sulfur mustard," *Pharmacol. Rev.* **48**, 289–326 (1996).
6. K. Kehe and L. Szinicz, "Medical aspects of sulphur mustard poisoning," *Toxicology* **214**, 198–209 (2005).
7. S. Khateri, M. Ghanei, S. Keshavarz, M. Soroush, and D. Haines, "Incidence of lung, eye, and skin lesions as late complications of 34,000 Iranians with wartime exposure to mustard agent," *J. Occup. Environ. Med.* **45**, 1136–1143 (2003).
8. R. Aghanouri, M. Ghanei, J. Aslani, H. Keivani-Amine, F. Rastegar, and A. Karkhane, "Fibrogenic cytokine levels in bronchoalveolar lavage aspirates 15 years after exposure to sulfur mustard," *Am. J. Physiol. Lung Cell. Mol. Physiol.* **287**, 1160–1164 (2004).
9. K. J. Smith and H. Skelton, "Chemical warfare agents, their past and continuing threat and evolving therapies. Part 1," *Skin Med.* **2**, 215–221 (2003).
10. P. Wilder-Smith, W. G. Jung, M. Brenner, K. Osann, H. Beydoun, D. Messadi, and Z. Chen, "*In vivo* optical coherence tomography for the diagnosis of oral malignancy," *Lasers Surg. Med.* **35**, 269–275 (2004).
11. P. Wilder-Smith, K. Osann, N. Hanna, N. El Abbadi, M. Brenner, D. Messadi, and T. Krasieva, "*In vivo* multiphoton fluorescence imaging: a novel approach to oral malignancy," *Lasers Surg. Med.* **35**, 96–103 (2004).
12. E. S. Matheny, N. M. Hanna, W. G. Jung, Z. Chen, P. Wilder-Smith, R. Mina-Araghi, and M. Brenner, "Optical coherence tomography of malignancy in hamster cheek pouches," *J. Biomed. Opt.* **9**, 978–981 (2004).
13. T. E. Milner, D. Dave, Z. Chen, D. M. Goodman, and J. S. Nelson, "OCT as a biomedical monitor in human skin," in *Optical Coherence Tomography*, R. R. Alfano and F. J. Alfano, Eds., pp. 220–223, W. B. Saunders Co., Philadelphia (1996).
14. K. J. Bamford, S. W. James, R. P. Barr, and S. Tatam, "Optical low coherence tomography of bronchial tissue," in *Advanced Materials and Optical Systems for Chemical and Biological Detection*, *Proc. SPIE* **3858**, 172–179 (1999).
15. C. Pitris, C. Jesser, S. A. Boppart, D. Stamper, M. E. Brezinski, and J. G. Fujimoto, "Feasibility of optical coherence tomography for high-resolution imaging of human gastrointestinal tract malignancies," *J. Gastroenterol.* **35**, 87–92 (2000).
16. A. Gautam, R. Vijayaraghavan, M. Sharma, and K. Ganesan, "Comparative toxicity studies of sulfur mustard (2,2′-dichloro diethyl sulfide) and monofunctional sulfur mustard (2-chloroethyl ethyl sulfide), administered through various routes in mice," *J. Med. Chem. Biol. Radiol. Defense* **4** (2006), accessed December 19, 2006, www.jmedcbr.org/issue_0401/Vijay/Vijay_02_06.html.
17. S. D. McClintock, G. O. Till, M. G. Smith, and P. A. Ward, "Protection from half-mustard-gas-induced lung injury in the rat," *J. Appl. Toxicol.* **22**, 257–262 (2002).
18. S. D. McClintock, L. M. Hoesel, S. K. Das, G. O. Till, T. Neff, R. G. Kunkel, M. G. Smith, and P. A. Ward, "Attenuation of half sulfur mustard gas-induced acute lung injury in rats," *J. Appl. Toxicol.* **26**, 126–131 (2006).
19. S. Gangolli, ed., "2-ethylthioethyl chloride," in *DOSE (Dictionary of Substances and Their Effects)*, 3rd electronic ed., Royal Society of Chemistry (2005). Last accessed February 9, 2010 at http://www.knovel.com/knovel2/Show_HTML_Text.jsp?BookID=527&SetID=6000659&TextID=0&Type=null&CurrentPage=1.
20. J. J. Salley, "Experimental carcinogenesis in the cheek pouch of the Syrian hamster," *J. Dent. Res.* **33**, 253–262 (1954).
21. J. H. Calvert, J. H. Jarreau, M. Levame, M. P. D'Ortho, H. Lorino, A. Harf, and I. Macquin-Mavier, "Acute and chronic respiratory effects of sulfur mustard intoxication in guinea pig," *J. Appl. Physiol.* **76**, 681–688 (1994).
22. D. R. Anderson, J. J. Yourick, R. B. Moeller, J. P. Petrali, G. D. Young, and S. L. Byers, "Pathological changes in rat lungs following acute sulfur mustard inhalation," *Inhalation Toxicol.* **8**, 285–297 (1996).
23. R. Vijayaraghavan, "Modifications of breathing pattern induced by inhaled sulfur mustard in mice," *Arch. Toxicol.* **71**, 157–164 (1997).
24. S. N. Dube, K. Husain, K. Sugerdran, R. Vijayaraghavan, and S. M. Somani, "Dose response of sulfur mustard: behavioral and toxic signs in rats," *Indian J. Physiol. Pharmacol.* **42**, 389–394 (1998).
25. D. D. Thorat, T. N. Mahadevan, and D. K. Ghosh, "Particle size distribution and respiratory deposition estimates of beryllium aerosols in an extraction and processing plant," *Am. Ind. Hyg. Assoc. J.* **64**, 522–527 (2003).
26. M. Sakagami, W. Kinoshita, K. Sakon, and Y. Makino, "Fractional contribution of lung, nasal, and gastrointestinal absorption to the systemic level following nose-only aerosol exposure in rats: a case study of 3.7 $\mu$m fluorescein aerosols," *Arch. Toxicol.* **77**, 321–329 (2003).
27. T. R. La Bone, "The new ICRP respiratory tract and systemic models," WSCR-MM-2000-0097 (2000). Retrieved August 6, 2004 at http://bidug.pnl.gov/references/wsrc-mm-2000-00097.pdf.
28. D. R. Anderson, S. L. Byers, C. R. Clark, and J. A. Schlehr, "Biochemical alterations in rat lung lavage fluid following acute sulfur mustard inhalation," *Inhalation Toxicol.* **9**, 43–52 (1997).
29. S. C. Pant and R. Vijayaraghavan, "Histochemical and histomorphological alterations in the lungs of mice following acute sulfur mustard inhalation," *J. Burns Surg. Wound Care* [serial online] **1**(1), 6 (2006), accessed December 19, 2006, http://www.journalofburns.com.